17th World Conference on Earthquake Engineering, 17WCEE

Sendai, Japan - September 13th to 18th 2020

PEAK GROUND VELOCITY AND COLLAPSE CHARACTERISTICS OF CFT FRAME

K. Goto[1]

[1] *Associate professor, National Institute of Technology, Kumamoto College, goto@kumamoto-nct.ac.jp*

Abstract

The basic object of earthquake resistant design of building structure is to prevent the collapse of building which have been observed in the recent sever earthquakes. In order to prevent the collapse of building and to design building on the basis of the ultimate state, the collapse behavior of building under extremely strong ground motion is required to be analyzed precisely.

It is well known that Concrete filled steel tube column (CFT column) is ductile and useful member as earthquake resistant element. However, in some cases CFT column fractures by the crack of steel tube under strong cyclic load like seismic load. This fracture is brittle and predicted to affect the whole collapse of frame. From this reason, seismic response collapse and crack damage of CFT frame, which is composed of CFT columns and I-section beams, had been investigated. Seismic response collapse of multi-story CFT frame is closely related to the failure of structural members, especially to failure of columns. Therefore, the restoring force characteristics and failure mechanism of CFT column caused by steel tube crack had been studied, and restoring force model and failure condition of it were obtained.

In this study, the frame damage and the collapse behavior of CFT frame under extremely strong earthquake are investigated in relation with the ultimate state design conditions (e.g. column overdesign factor, number of stories and concrete-to-tube strength ratio of CFT column). In the seismic response analysis of CFT frame, multi-story plane frame is assumed to be composed of the rigid panel zones of beam-to-column connection and the axially elastic members with elastic-plastic hinges at both ends. The restoring force model of elastic-plastic hinge had been obtained on the basis of the dynamic loading tests of CFT column.

The numerical analysis method to predict the damage of CFT frame is obtained by introducing the damage ratios of the steel tube crack of CFT column and the crack fracture of I-section beam. By the use of the presented analysis method, the ultimate damage situation of CFT frame designed under quite different design condition is calculated and relation between the collapse behavior of CFT frame and peak ground velocity when the frame collapses are obtained quantitatively on the ultimate state design condition in this paper.

Keywords: Concrete filled steel tube, Multi story frame, Crack, Collapse, Peak ground velocity

1. Introduction

Recently, the great earthquake that several big earthquakes happen in succession is predicted in Japan. In particular, an ocean-trench-type earthquake, which is predominant in long period ground motion, is also predicted. The predicted earthquake size was changed after the 2011 Tohoku Earthquake, and the earthquake response analyses with building collapse under extremely strong earthquake spread immediately. To analysis the response of building under extremely strong earthquake, it is necessary to consider the quantitative assessments of fracture, strength degradation behavior of members and the analysis considered the P-Δ effect of frame in large deformation range. However, we do not have the enough knowledge on concrete filled steel tube (CFT) structure to such problems because CFT structure shows excellent earthquake resistant performance as compared with the other structures. This situation is very dangerous because of the circumstance with the unclear maximum excitation of earthquake. CFT structure is often adopted in the super high-rise building which has long natural period. It is predicted that CFT structure under ocean-trench-type earthquake suffers the severe damage which is caused by large and a lot of repeated plastic deformations. Accordingly, it is very important to study the collapse behavior of CFT structure.

In this study, the relations between peak ground velocity (PGV) of input ground motions and the crack of CFT column and collapse of CFT frame are investigated in relation to the ultimate state design conditions. The numerical analysis method to predict the damage of CFT frame is obtained by introducing the damage ratios of the steel tube crack and local buckling of CFT column and the crack fracture of I-section beam [1]. Using the presented analysis method, the ultimate damage situations of CFT frames designed under quite different design conditions are calculated and relations between the collapse behavior of CFT frame and peak ground velocity when the frame collapses are obtained quantitatively on the ultimate state design conditions in this paper.

2. Analyzed CFT frames

Calculated CFT frames are from 2-story to 15-story frames whose span number is 3 in this study. They are designed under the following conditions.

i) The distribution of story shear strength is decided by the Japanese design code. The base shear strength (C_B) of frame is decided by the deformation limit condition of it, and $C_B = \beta \cdot W$. β is the base shear coefficient, and it is shown in Fig. 1. W is the total weight of frame. This frame strength is calculated by the limit analysis assuming the weak-beam type frame, which has the collapse mechanism of frame with plastic hinges at every beam-end and the upper and lower column-ends in the top story and the first story.

ii) It is well known that the column overdesign factor (r_{cb}) is an important earthquake resistant design factor of multi-story frame. To ensure that a frame structure collapses according to the beam-hinging pattern, the columns are generally overdesigned with r_{cb}. For multi-story frame, r_{cb} is defined for each beam-to-column connection as the ratio between the sum of the column strength and the sum of the beam strength at that node, as shown in Eq. (1).

$$r_{cb} = (\Sigma\ {}_cM_u)/(\Sigma\ {}_bM_u) \tag{1}$$

where ${}_cM_u$, ${}_bM_p$ are the ultimate moment and the full plastic moment of the columns and beams, respectively.

iii) The strength ratio of filled concrete to steel tube (ρ, $\rho = \sigma_c A_c / \sigma_u A_s$, σ_c: the compression strength of filled concrete, σ_u: the tensile strength of steel tube, A_c, A_s: the sectional area of filled concrete and steel tube respectively) affects the restoring force characteristics of CFT column strongly [2]. From this reason ρ of all CFT columns are assumed to be the same and they are $\rho = 1$ in this study.

iv) Every I-section beam of multi-story frame satisfies the critical conditions of the width-to-thickness ratio of flange (b/t_f) and web (h/t_w) and the lateral buckling parameter ($L_b h/A_f$). They are $b/t_f = 5$, $h/t_w = 71$ and

$L_b h/A_f$ = 375 (b: half width of flange, h: depth of beam, t_f, t_w: thicknesses of flange and web respectively, A_f: sectional area of flange, L_b: beam length).

All CFT frames are designed under the conditions mentioned above and another condition that any dimensions of steel tube and I-section is available.

Story-height of every CFT frame is 4.0 m and the span lengths of outer span and inner span are 8.0 m and 6.0 m respectively. The weight of each story is 2000 kN. The yield stress (σ_y) and the tensile strength (σ_u) of steel tube and I-section beam are σ_y = 340 N/mm^2 and σ_u = 440 N/mm^2. The fracture elongation (ε_f) of steel tube and I-section beam is ε_f = 0.20. The compression strength of filled concrete (σ_c) is σ_c = 60 N/mm^2.

Some results of designed CFT frames are shown in Fig. 2 – 3 in which there are natural periods (T), diameters (D) of CFT column and depths (h) of I-section beam at the first story. The design conditions of CFT frames are quite different among them. However, every diameter (D) of CFT column and depth (h) of I-section beam is practical dimension.

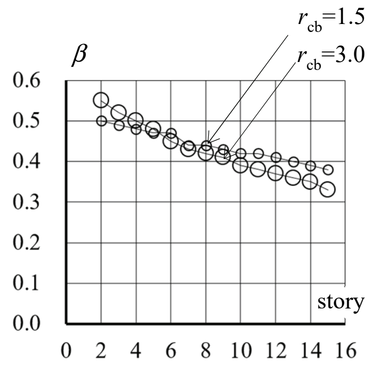

Fig. 1 – Base shear coefficient

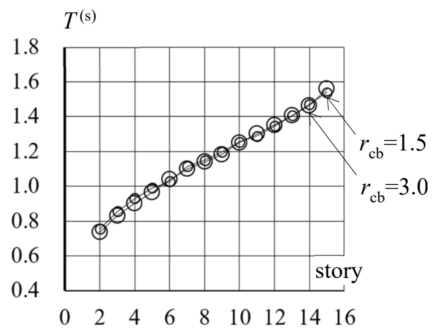

Fig. 2 – Natural period

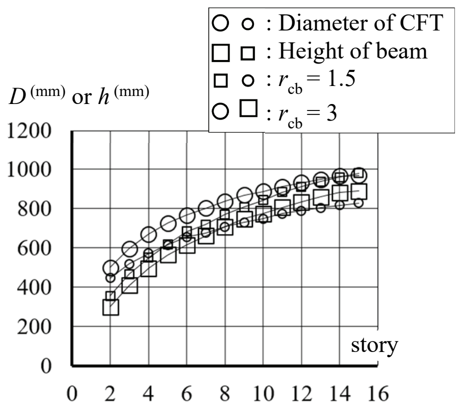

Fig. 3 – Diameter of CFT column and height of I-section beam at 1st story

3. Seismic response analysis

3.1 Multi-story CFT frame model

In the seismic response analysis of CFT frame, multi-story plane frame is assumed to be composed of the rigid panel zones of beam-to-column connection and the axially elastic members with elastic-plastic hinges at both ends as explained in Fig. 4. This assumption related to the rigid panel zone can be satisfied in most real CFT frames because the steel beam to CFT column moment connection has large shear strength. The mass of frame is concentrated in every panel zone and distributed uniformly in it. The displacement of frame can be expressed only by the rotation, the horizontal displacement and the vertical displacement of every rigid panel zone. The viscous damping of frame is expressed by the Rayleigh damping in which the damping ratios of the first mode (h_1) and the second mode (h_2) are assumed to be h_1 = 0.02, h_2 = 0.02.

3.2 Restoring force model of CFT column and I-section beam

The restoring force model of elastic-plastic hinge is obtained on the basis of the dynamic loading tests of CFT column [2]. According to the test results the non-dimensional restoring force (M/M_u) of CFT column until the local buckling of steel tube is approximated by the Tri-linear model whose skeleton curve is explained in Fig. 5 (a). After the local buckling of steel tube, it is expressed by the Clough model [3] as shown in Fig. 5 (b). The stiffness ratios in the plastic range in Figs. 5 (a)-(b) are given as K_1/K_0 = 0.2, K_2/K_0 = 0.001 which are approximated on the basis of the test results [2]. The restoring force models mentioned above are defined by the non-dimensional restoring force (M/M_u) in which the ultimate bending strength (M_u) changes at every moment by the varying axial force of CFT column. Accordingly, the restoring force model can simulate the

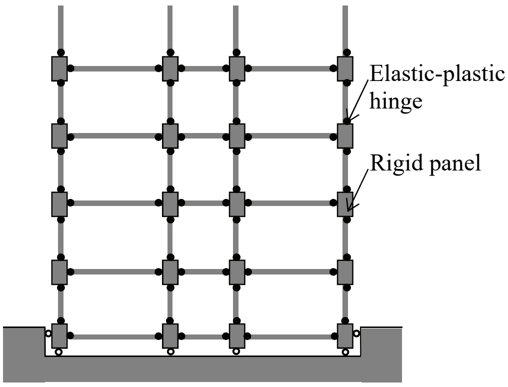

Fig. 4 – CFT frame model

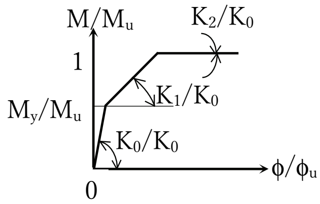

(a) Before local buckling
(K_1/K_0=0.2, K_2/K_0=0.001)

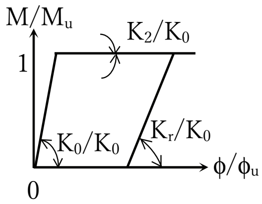

(b) After local buckling
(K_2/K_0=0.001)

Fig. 5 – Restoring force model of CFT column

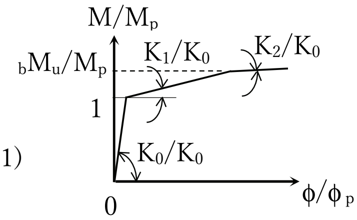

(K_2/K_0=0.001, ϕ_p=M_p/K_0)

Fig. 6 – Restoring force model of I-section beam

effect of varying axial force of CFT column. M_u is obtained by the generalized superposed strength method considering the confined effect [2].

I-section beam of multi-story CFT frame is also expressed by the axially elastic member with the elastic-plastic hinges at both ends as shown in Fig. 3. The restoring force of the elastic-plastic hinge is decided by the Tri-linear model shown in Fig. 5 in which the restoring force characteristics are given by the full plastic moment (M_p) and the ultimate bending strength of I-section beam (${}_bM_u$). The strain hardening behavior of I-section beam affects the seismic response and collapse of CFT frame under strong ground motion. Accordingly, the strain hardening of I-section beam in the model cannot be neglected. It is given by the value K_1 which is obtained by assuming I-section beam is approximated by two-flange section member.

$$K_1/K_0 = (1/y - 1)/\{1.5y\,(1 - y)(1 + u) - 1\} \tag{2}$$

where y (= σ_y/σ_u) and u (= $\varepsilon_u/\varepsilon_y$) mean the yield stress ratio and the ultimate tensile strain ratio respectively.

3.3 Input ground motion

To calculate the dynamic collapse of CFT frame, the recorded strong ground motions and the artificial ground motions are used as input ground motion. The recorded strong ground motions are El Centro (1940) NS, Taft (1952) EW, Hachinohe (1968) NS and JMA-Kobe (1995) NS. The characteristics of input ground motions and pseudo-velocity response spectra are shown in Table 1 and Fig. 7.

3.4 Collapse analysis method

To analyze the dynamic collapse behavior of CFT frame, the following conditions are used for calculation.

i) After the crack of CFT column or I-section beam, the restoring force and the stiffness of the elastic-plastic hinge is lost linearly and fully in 0.1 second.

ii) The stress redistribution after the crack is expressed by distributing the holding stress of elastic-plastic hinge to the stress components of the panel zone in both members' ends.

Table1 – Input ground motion

Type	Notation	Earthquake	PGA (m/s^2)	PGV (m/s)	Duration (s)
Recorded wave	ELC	El Centro (1940) NS	3.42	0.336	54
	TAF	Taft (1953) EW	1.76	0.165	54
	HAC	Hachinohe (1968) NS	2.30	0.340	51
	KOB	JMA-Kobe (1995) NS	8.21	0.900	32
Artifficial wave	BCJ	BCJ-L2	3.56	0.521	120
	NOT1	Notice 1	5.53	0.794	82
	NOT2	Notice 2	5.61	0.739	82
	NOT3	Notice 3	5.59	0.859	82

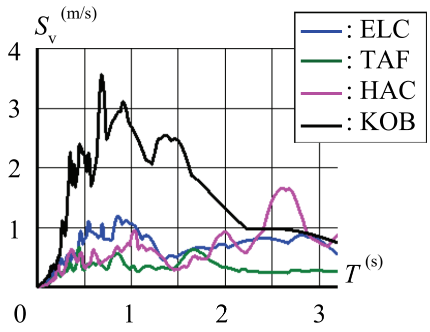

(a) Recorded ground motion

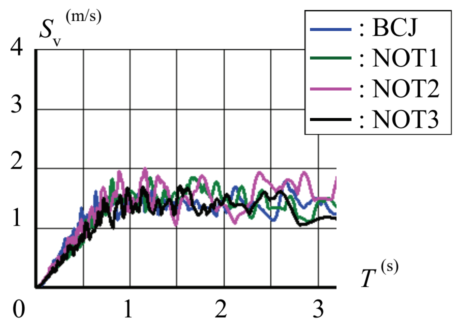

(b) Artificial ground motion (PGV = 0.5 (m/s))

Fig. 7 – Pseudo-velocity spectrum of input ground motion

iii) In falling down process, the collision force between the upper and lower rigid panels of the beam-column connection is given by the compression load – deformation relation obtained the stub-column tests of CFT column.

4. Damage ratio of CFT column and I-section beam

4.1 Damage ratio of CFT column

From the cyclic loading tests of CFT column it is shown that the steel tube of CFT column cracks and fractures when the accumulated plastic strain of steel tube becomes to be equal to the critical value ($\alpha\varepsilon_f$). From this result, the cracking condition of CFT column is expressed by Eq. (3) [2].

$$\Sigma\varepsilon_{TC} + \Sigma\varepsilon_T = \alpha\varepsilon_f \tag{3}$$

where ε_T : the plastic tension strain of steel tube in the tension stress side. ε_{TC} : the plastic tension strain due to the local buckling deformation of steel tube in the compression stress side. α (= –0.3ρ + 5.0) : constant expressed by the strength ratio of filled concrete to steel tube (ρ), ε_f : fracture elongation of steel tube, Σ :

summation of plastic strain under cyclic load. From Eq. (3), the cracking damage ratio of CFT column (${}_{c}D_{cr}$) is expressed by Eq. (4).

$${}_{c}D_{cr} = (\Sigma\varepsilon_{TC} + \Sigma\varepsilon_{T})/\alpha\varepsilon_{f} \tag{4}$$

As shown in Eq. (3), the local buckling of steel tube is closely related to the steel tube cracking. The local buckling condition is obtained on the basis of the upper bound theorem of the limit analysis [4]. The damage ratio of local buckling (${}_{c}D_{lb}$) is decided to use critical deformation (${}_{c}\delta_{lb}$) that corresponds to the CFT column deformation for the steel tube to buckle locally.

$${}_{c}D_{lb} = ({}_{c}\delta_{PC} - {}_{c}\delta_{PT})/{}_{c}\delta_{lb} \tag{5}$$

where (${}_{c}\delta_{PC}$ − ${}_{c}\delta_{PT}$) is the amplitude of plastic deformation of CFT column. Using Eqs. (3)–(4), the local buckling and the steel tube cracking in the restoring force of CFT column mentioned above are decided.

4.2 Damage ratio of I-section beam

When strong alternating repeated load is applied to the I-section cantilever beam, flange buckles locally and after that cracks even if the fracture at the welded joint is avoided. According to the dynamic loading tests of I-section cantilever beam, the cracking fracture of I-section beam is considered as the very low-cycle fatigue behavior and assumed to be approximated by the Palmgren-Miner rule [5, 6]. From the Palmgren-Miner rule, the damage ratio is given by the accumulation of each cycle damage [7]. Therefore, the cracking damage ratio of I-section beam (${}_{b}D_{cr}$) in each instant under random repeated load can be expressed by Eq. (6).

$${}_{b}D_{cr} = \Sigma_{j}\,(1/N_{fj}) \tag{6}$$

where N_{fj} means the number of cycles to fracture under j-th cycle load and N_f is approximated by the Coffin-Manson relationship as shown in Eq. (7).

$$\varepsilon_{pa} = \varepsilon_{f}\,(2N_f)^{c} \tag{7}$$

where ε_{pa}: the plastic strain amplitude of I-section beam flange buckled locally [6], ε_f : fracture elongation, c: material modulus.

The local buckling condition of flange at the beam end is obtained on the basis of the upper bound theorem of the limit analysis [5]. The damage ratio of local buckling (${}_{b}D_{lb}$) is decided by the use of critical deformation (${}_{b}\delta_{lb}$).

$${}_{b}D_{lb} = ({}_{b}\delta_{PC} - {}_{b}\delta_{PT})/{}_{b}\delta_{lb} \tag{8}$$

5. Collapse behavior and peak ground velocity

5.1 Monotonic horizontal loading analysis with frame collapse

Static analyses under monotonic horizontal load have been carried out. The calculated load – deformation relations of 5, 10 and 15-story frames are shown in Fig. 8. The vertical axis is the load expressed by (Q_1/W)/β. Q_1 is the story shear force of the first story, W is the total weight of frame and β is the target base shear coefficient shown in Fig. 1. The horizontal axis is the frame deformation expressed by the ratio of the horizontal deformation of the top floor (u_{top}) and height of frame (L_H). From calculated results, it is shown that the maximum frame strength of each frame almost reached the target strength and the load deterioration after maximum strength is caused by the P-Δ effect of frame. However, the extremely load deterioration is caused by the cracks of members. Moreover, the energy dissipation until frame collapse is affected by the column overdesign factor (r_{cb}) strongly.

Final frame deformations when the horizontal load is lost perfectly are shown in Fig. 9. In case of frames of r_{cb} = 3.0, it is confirmed that the collapse mechanism is the weak beam type supposed in frame design. However, in the case of frame of r_{cb} =1.2, the collapse mechanism is not the weak beam type because the damage concentrations occur in columns at middle to upper stories.

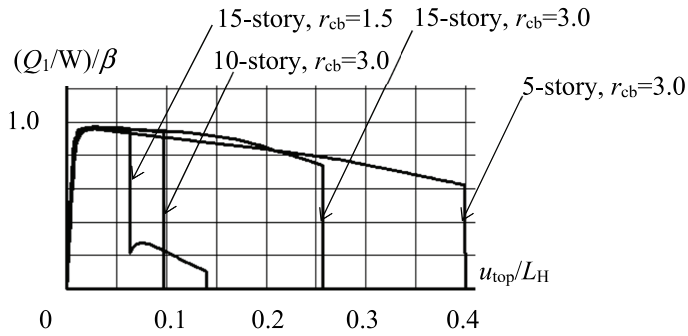

Fig. 8 – Load – deformation relation of CFT frame under monotonic horizontal load

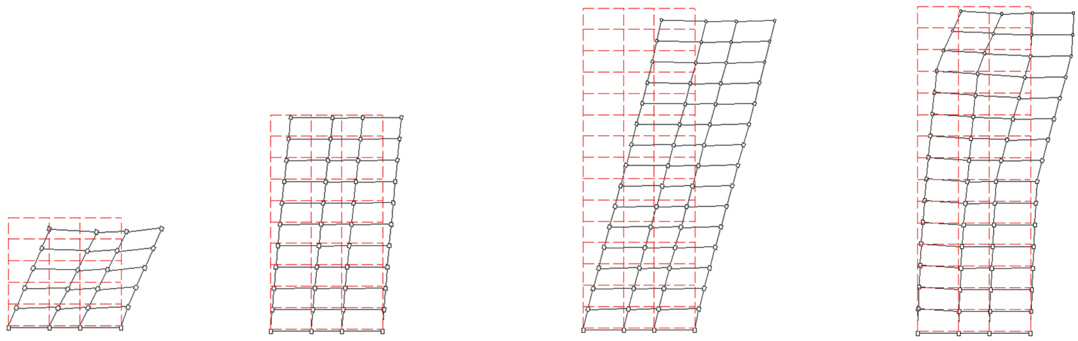

(a) 5-story, r_{cb}=3.0 (b)10-story, r_{cb}=3.0 (c)15-story, r_{cb}=3.0 (d)15-story, r_{cb}=1.5

Fig. 9 – Final frame deformation under monotonic horizontal load

5.2 Seismic response analysis with frame collapse

Dynamic collapse behaviors of CFT frames under extremely strong ground motion have been carried out. The input ground motion is BCJ-L2 whose peak ground velocity (PGV) is amplified to PGV = 1.4 m/s. Frame deformations and damage distributions when calculation had been completed are shown in Fig. 10. Frame deformation shown in Fig. 10 is the seismic response deformation in every 10 seconds. Damage shown in Fig. 10 is the local buckling damage ratio (${}_cD_{lb}$, ${}_bD_{lb}$) and the crack damage ratio (${}_cD_{cr}$, ${}_bD_{cr}$). These damage ratios are expressed by the length of thick lines perpendicular to the axis of column and beam. The numerical values in the figures explain the damage ratios of CFT columns in the first story and the top story. Red lines show that the damage ratio equal to be 1.0, that is, the local buckling or the crack occurs in CFT column or I-section beam.

Although all CFT frames are designed under the same condition of weak-beam type frame, the local buckling and crack damage appear in some CFT columns because of an effect of response with high-order natural vibration mode and the varying axial force of CFT column, which changes the ultimate bending strength (${}_cM_u$) of CFT column.

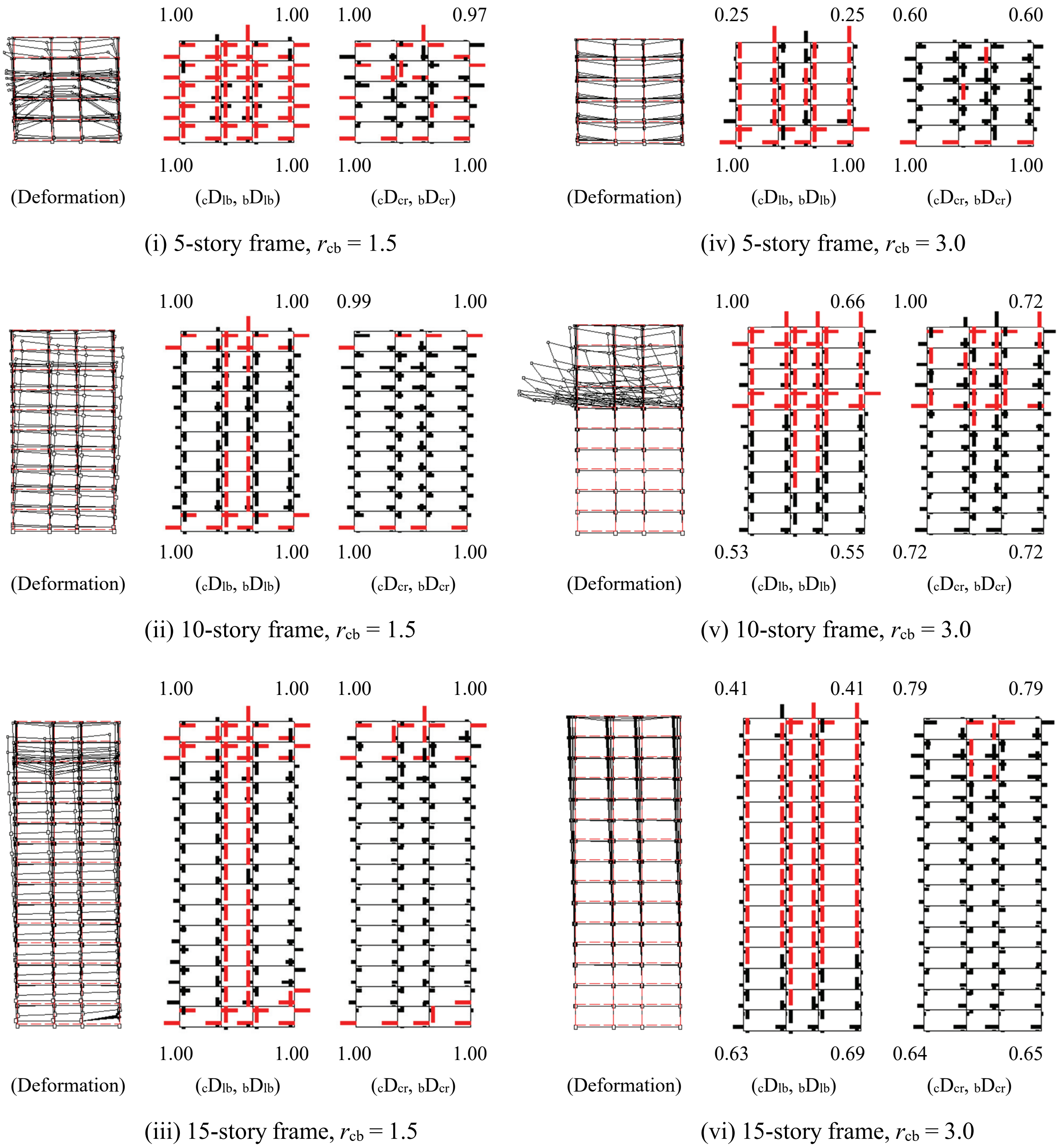

Fig. 10 – Frame deformation and damage distributions of CFT frame under extremely strong earthquake (BCJ, PGV = 1.4 m/s)

Fig. 11 shows the converted velocity (V_{dm}) of the input energy causing damage (E_{dm}) and the vertical displacement at uppermost story (w_{top}). V_{dm} and E_{dm} are expressed by Eqs. (9)–(10).

$$E_{\mathrm{dm}} = E_{\mathrm{e}} + E_{\mathrm{p}} - E_{\mathrm{g}} \tag{9}$$

$$E_{\mathrm{dm}} = 0.5\, M\, V_{\mathrm{dm}}^2 \tag{10}$$

where E_{e} is the elastic strain energy, E_{p} is the energy dissipation by plastic deformation at elastic-plastic hinges, E_{g} is the gravitational potential energy and M is total mass of frame.

The solid lines and dashed lines in Fig. 11 show times of the column crack and beam crack respectively. Timing information when the story collapse occurs and record the maximum V_{dm} is also shown as $T_{4\mathrm{cr}}$ and T_{Vdm} respectively in Fig. 11. A figure in 【 】 shows the collapse story. As shown in Fig. 11, in case of 4-story frames, the story collapse occurs at the first story, and V_{dm} decreases drastically after that. Moreover, the story collapses occur in the second story and the 4th story after V_{dm} becomes zero in frame of $r_{\mathrm{cb}} = 1.5$. In case of 9-story frame of $r_{\mathrm{cb}} = 1.5$, V_{dm} hardly decreases after the story collapse in uppermost story. On the other side, in case of $r_{\mathrm{cb}} = 3.0$, V_{dm} decreases drastically after the first story collapse. In case of 12-story frame of $r_{\mathrm{cb}} = 3.0$, V_{dm} increases although many beam cracks occur.

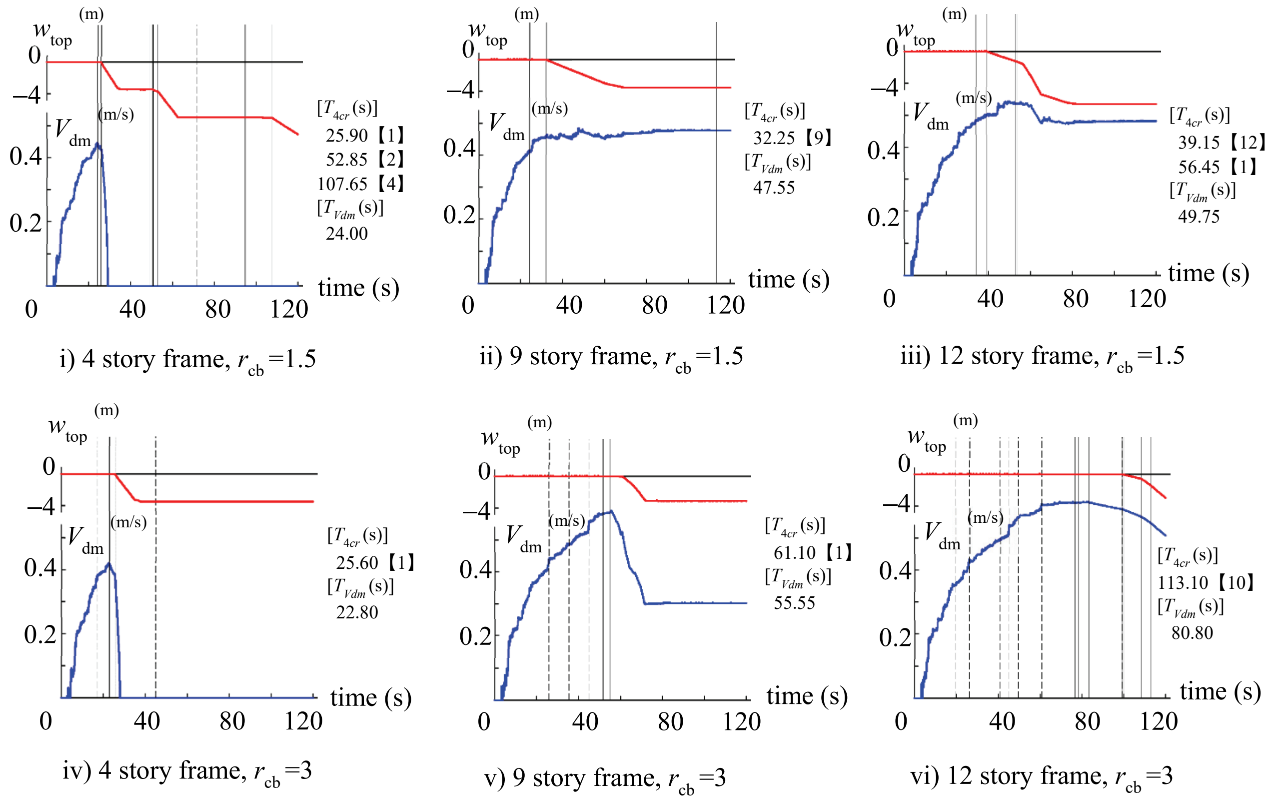

Fig. 11 – Vertical displacement at uppermost story and input energy causing damage of CFT frame under extremely strong earthquake (BCJ, PGV = 1.4 m/s)

6. Peak ground motion

Peak ground velocities (PGV) when the first crack occurs in CFT column and I-section beam and the story collapse occurs are shown in Fig. 12. PGV is set every 0.1 m/s in seismic response analysis. PGV that the story collapse occurs is varied due to the input ground motions and the number of stories complicatedly. However, in general, the story collapse of CFT frame with r_{cb} = 3.0 requires more PGV values than CFT frame with r_{cb} = 1.5. In addition, the column cracks and story collapses occur at relatively close PGV, however the beam cracks are often farther than the story collapses. In other words, the beam crack does not affect to the story collapse.

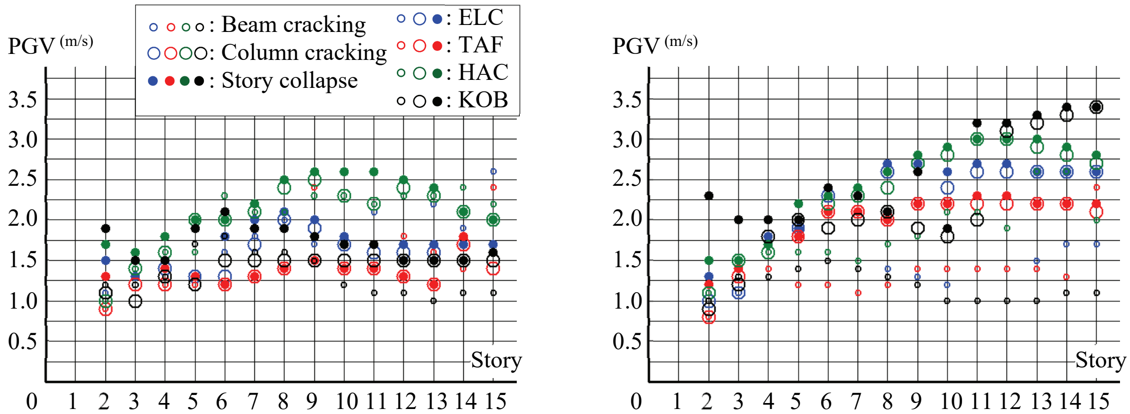

i) r_{cb} =1.5 ii) r_{cb} =3.0

(A) Recorded strong ground motion

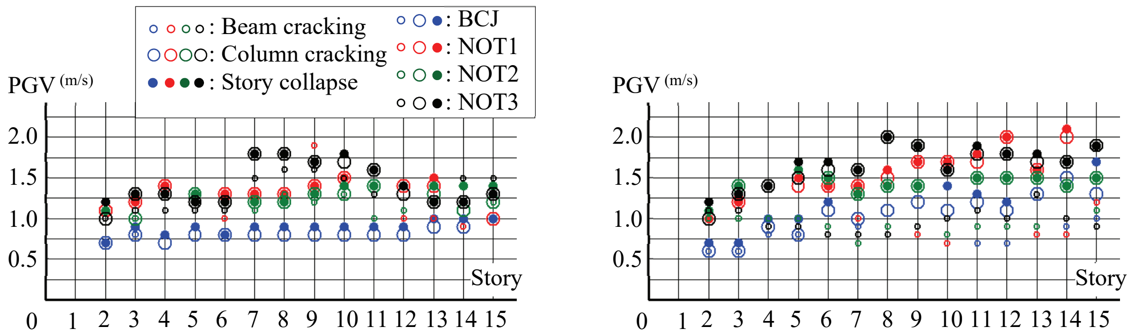

i) r_{cb} =1.5 ii) r_{cb} =3.0

(B) Artificial strong ground motion

Fig. 12 – PGV when the first crack occurs in CFT column and I-section beam and the story collapse occurs

7. Conclusions

The collapse behaviors and the damage of CFT frame under extremely strong earthquake are obtained by introducing the damage ratios of local buckling and crack of CFT column and H-section beam. From the numerical analysis, it is pointed out that not only the ultimate strength of frame and the strength distribution along the story but also the column overdesign factor affects the collapse behavior and the damage ratio of member strongly.

Moreover, collapse behaviors of CFT frame from 2-story to 15-story and the converted velocity of the input energy causing damage (V_{dm}) are also investigated in this study. V_{dm} decreases drastically when the first story collapse occurs. However, V_{dm} hardly affected the uppermost story collapse, and the beam crack does not affect to the change of V_{dm}.

PGV that the story collapse occurs is varied due to the input ground motion and the number of stories. However, in general, the story collapse of CFT frame with r_{cb} = 3.0 requires more PGV values than CFT frame with r_{cb} = 1.5.

References

[1] Goto K (2012): Seismic response and damage limit of concrete filled steel tube frame, *Proceedings of the 14th International Symposium on Tubular Structures*, U.K., 533-539.

[2] Saisho M and Goto K (2001): Restoring force model of concrete filled steel tube column under seismic load, *Proceedings of the 9th Pacific Structural Steel Conference*, China, 453-458.

[3] Clough, R.W. & Johnston, S.B. (1966): Effect of Stiffness Degradation on Earthquake Ductility Requirements. *Proceedings of Japan Earthquake Engineering Symposium*: 227-232.

[4] Saisho M, Kato M, and Gao, S (2004). Local buckling of CFT-column under seismic load, *Proceedings of the 13th World Conference on Earthquake Engineering*, Paper No.2614., Canada, 1-15.

[5] Goto K (2010): Crack fracture type of I-section cantilever beam under strong cyclic load, *Proceedings of 9th Pacific Structural Steel Conference*, China, 1017-1023.

[6] Goto K and Saisho M, 2010 (2010): Crack damage of multi-story CFT frame under strong motion, *Proceedings of the 13th International Symposium on Tubular Structures*, Hong Kong, 149-157.

[7] Dowling, N.E. (2007). *Mechanical Behavior of Materials*, New Jersey: Person Prentice Hall.

[8] Goto K (2015): Seismic response and damage distribution of concrete filled steel tube frame, *Proceedings of the 15th International Symposium on Tubular Structures*, Rio de Janeiro, 157-163.

[9] Goto K (2016): Crack collapse and column overdesign factor distribution of CFT Frame, *Proceedings of the 8th International conference on Steel and Aluminum Structures*, Hong Kong, Paper No.139, 1-11.

[10] Saisho M and Goto K (2004): Ultimate earthquake resistant capacity of CFT-frame, *Proceedings of the 13th World Conference on Earthquake Engineering*, Paper No.2613., Canada, 1-15.

